Effects of Rotor-Rotor Interactions on Aerodynamic Loads for Two Helicopters in Forward Flight

Oznur Yemenici
oyemenici@tai.com.tr
Department of Aerospace Engineering,
Middle East Technical University (METU),
Ankara, Turkey

Nilay Sezer Uzol
nsezeruzol@etu.edu.tr
Department of Mechanical Engineering,
TOBB University of Economics and Technology,
Ankara, Turkey

Oguz Uzol
uzol@metu.edu.tr
Department of Aerospace Engineering,
Middle East Technical University (METU),
Ankara, Turkey

ABSTRACT

This paper presents an investigation of the aerodynamic interactions between two UH-1H helicopter rotors in forward flight. The wake flow structure and performance characteristics of the rotors are investigated when the rear rotor is operating within the wake of the front rotor. A 3-D unsteady vortex-panel method potential flow solver based on a free-vortex-wake methodology is used for this purpose. The solver is validated using the experimental data from the Caradonna-Tung experiments. The interactional analyses are performed for 10 different positions of the rear rotor with respect to the front rotor. The wake of the front rotor, which is generated due to the mutual interactions of the wake and tip vortices, is significantly asymmetric and non-uniform. Therefore the rear rotor operates within a complex and vortical free-stream flow. The wake-rotor interactions cause substantial variations in the forces generated by the rear rotor. The asymmetries in the wake geometry in forward flight cause changes in performance characteristics of the rear rotor when it is operating at the retreating and advancing sides of the front rotor. The decrease in vertical lifting is more when the rear rotor is operating within the wake of the advancing side. A frequency spectrum analysis of the force and moment fluctuations of the rear rotor shows that for the vertical force component the rear rotor experiences a dominant peak at two times the blade passing frequency, except when the rear rotor is operating within the wake of the advancing side of the front rotor. Other peaks at different harmonics are also observed and the location of these peaks in the frequency spectrum depends on the lateral position of the rear rotor with respect to the front one. Moment fluctuations generally are similar for the front and rear rotors except for the pitching moment which show fluctuations at two times the blade passing frequency illustrating that the pitching moment gets influenced by the wake interactions more than the other two moment components.

I. Introduction

Helicopter rotor flow fields with their three-dimensional and unsteady nature are one of the most complex and hard-to-predict flows in aerodynamics. The interactions with other rotor systems or with non-rotating components like the fuselage add to the complexity. The wake of a helicopter rotor is dominated by concentrated vortices trailing at the blade tips as well as vorticity shed from the blade surfaces [1]. Accurate modeling of this complex flow plays a crucial role for determining the performance characteristics and predicting the loads on the rotor blades.

Many different problems in interactional aerodynamics in helicopters have been investigated both experimentally and computationally by previous researchers. Experiments by Bi and Leishman [2], Wilson and Mineck [3], Sheridan and Smith [4], Smith and Betzina [5] and McMahon et al. [6] have shown that the rotor wake induces pressure loads on the fuselage. Wilby et al. [7] and Betzina et al. [8] have shown that the airframe also affects the loads and performance of the main rotor. Fletcher and Brown have emphasized that the main rotor wake causes both unsteadiness and nonlinearity to the tail rotor performance [9]. Meakin has simulated the streakline patterns for the V-22 Tiltrotor (operating in the helicopter mode) [10]. Akimov et al. [11] have emphasized the interacting wake structure of a coaxial Kamov Ka-32 helicopter with smoke injection near the tips of the rotor blades for different advance ratios. Bagai and Leishman [12] have used this experimental data to compare the wake prediction of their free-wake code. Brown [13] has used both results to verify his computational rotor wake model based on the numerical solution of the unsteady fluid-dynamic equations.

This paper presents an investigation of the aerodynamic interactions between two UH-1H helicopter rotors in forward flight. The impact of these interactions on the performance characteristics of the two rotors is investigated when the rear rotor is operating within the wake of the front rotor. A 3-D unsteady vortex-panel

method potential flow solver based on a free-vortex-wake methodology is used for this purpose. The solver is validated using the experimental data from the Caradonna-Tung experiments. The interactional analyses are performed for 10 different positions of the rear rotor with respect to the front rotor. The complex and asymmetric wake flow structure due to the mutual interactions of wake and tip vortices are demonstrated and the resultant variations of the rotor forces and moments are presented.

II. Methodology

The computations are performed using a three-dimensional unsteady free-wake vortex panel method code, developed by the authors. This code allows any number and any combination of fixed and/or rotating wings as well as non-lifting bodies to be included in the solution domain. All solid bodies in the domain are discretized using quadrilateral panel elements, and vortex ring elements are placed within each element. Once the vortex strengths of each vortex ring are obtained as a result of the solution at each time step, the blades are moved according to their respective kinematic motion to the next time step, and a row of wake panels are shed from the blade trailing edges with vortex strengths being equal to the difference between the suction and pressure side panels at the trailing edge, hence satisfying the unsteady Kutta condition at the trailing edge. These wake panels maintain their strengths in time, they are allowed to deform freely and interact with each other and are transported with the local flow velocity at each time step. The vortex rings on blade surfaces and in the wake panels, each one induces a velocity on each other, the magnitude of which is calculated also using the Biot-Savart law. Since the Biot-Savart law is singular for r→0, various vortex core models are implemented in the code, such as the Rankine [14], Vatistas [15], Scully [16] and Oseen-Lamb [17] models. This code is previously validated against various test cases including the Caradonna-Tung rotor test case [18, 19] as well as the NREL Phase VI wind turbine experiments [20].

For a more accurate blade loading prediction in forward flight, trim conditions are also implemented in the code. The trim conditions are obtained through a flight control system as explained in [21]. The blade flapping motion is defined as

$$\beta(\psi) = \beta_0 + \beta_{1c} Cos(\psi) + \beta_{1s} Sin(\psi) \quad (1)$$

where β_0 is the precone angle, β_{1c} is the longitudinal Tip Path Plane angle and, β_{1s} is the lateral Tip Path Plane angle. The blade pitching motion is defined as

$$\theta(\psi) = \theta_0 + \theta_{1c} Cos(\psi) + \theta_{1s} Sin(\psi) \quad (2)$$

where θ_0 is the collective pitch angle, θ_{1c} is the lateral cyclic pitch angle and θ_{1s} is the longitudinal cyclic pitch angle. Using the trim values for the β and θ angles for each forward flight condition, the blade pitch and flapping motions are computed as a function of the azimuth angle at each time step of the solution and the wake shedding process is performed according to the local position of the blade at that azimuth angle.

III. Results

In the first part of this section, the results of the simulations for the Caradonna-Tung rotor test case [22] are presented for the validation of the solver. The second part presents results from UH-1H rotor interaction simulations in various forward flight conditions.

A. Simulations for Code Validation:

The Caradonna-Tung rotor has two blades with no twist, no taper, 1.143 m radius and an aspect ratio of 6 with a NACA 0012 airfoil section operating in hover. The collective angle is set to 8° and the rotational speed is 1250 rev/min, which results in a 0.44 Mach number at the tips. The rotor blade surfaces are discretized by 40 chordwise and 10 spanwise panels. The blade rotations are impulsively started and the time increment is chosen such that the rotor blades advance 6° at each time step therefore one revolution is completed in 60 time steps. Figure 1 shows the structure of the wake behind the rotor and the surface pressure distribution at 80% radius station after 30 rotor revolutions. There's reasonable agreement with experimental data. More comparisons can be found in [19].

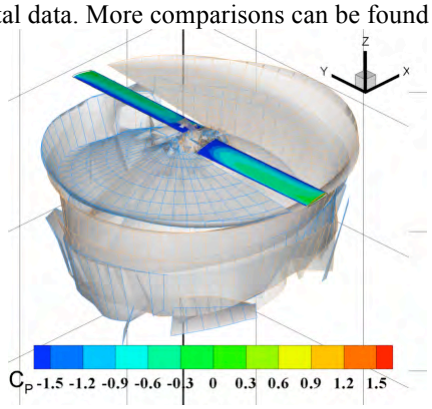

a)

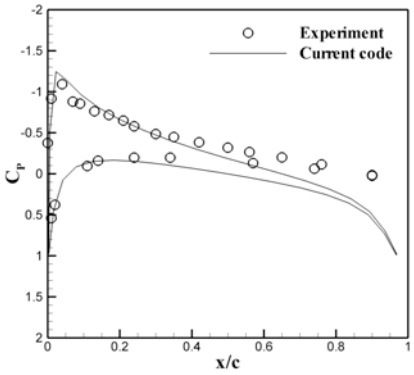

b) r/R =0.80

Figure 1. *Caradonna-Tung rotor simulation a) wake structure b) comparison of chordwise C_P distribution on r/R=0.80* [19]

B. Simulations of interactions between two UH-1H Rotors:

The interaction analyses are performed for ten different locations of the rear rotor as presented in Figure 2. In Case 1, the distance between the hub centers is 24.7 m, which corresponds to the case where the hub center of the rear rotor is 1 diameter away from the tail of the front

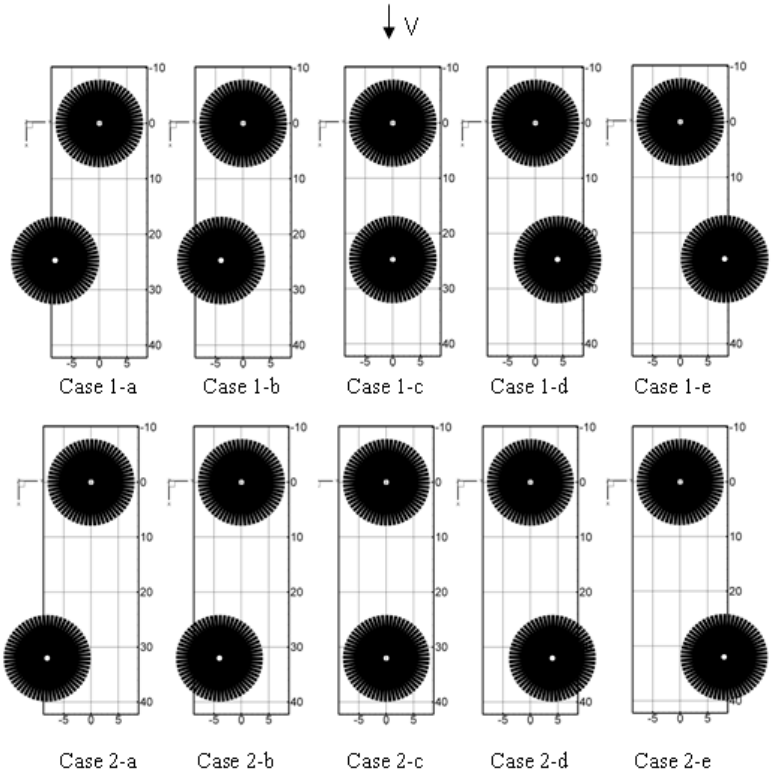

Figure 2. *Top views of the two UH-1H rotors showing the computational cases for interactional analysis: Case 1-a → Case 1-e show 5 different locations of the rear rotor in y-direction (lateral direction) when the difference between hub centers is 24.7m, Case 2-a → Case 2-e show 5 different locations of the rear rotor in y-direction when the difference between hub centers is 32 m. All dimensions are in meters.*

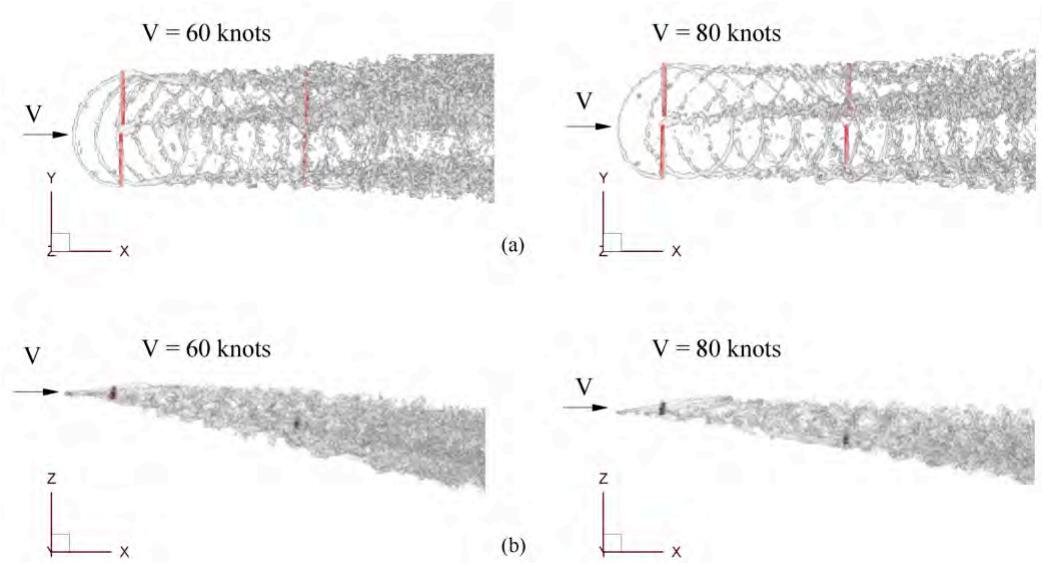

Figure 3. *Iso-vorticity surfaces showing tip and root vortex structures and the wake geometry behind UH-1H rotors comparing 60 knots and 80 knots forward flight conditions after 10 rotor revolutions (Simulation of Case 1-c): (a) Top view, (b) Side view* [19]

helicopter. In case 2, the distance between the hub centers is 32.0 m, in which the rear rotor is 1 additional radius away from the front rotor. In all cases the rear rotor is located slightly lower than the front rotor to make sure it will be operating within the wake flow field of the front rotor.

The aerodynamic interactions between the two rotors cause complex wake-rotor interactions, the results of which are presented in our previous publications [19]. Figure 3 presents a sample view of the flow structure using iso-vorticity surfaces after both rotors have completed ten revolutions.

In this paper we concentrate more on the effect of wake-rotor interactions on the performance characteristics of the rear rotor, i.e. the unsteady force and moment variations. As a part of the computation, time histories of all forces (F_X, F_Y, F_Z,) and all moments (M_X, M_Y, M_Z) are calculated. Figure 4 shows the time history of only the vertical force (F_Z) for both the rear and the front rotor over ten rotor revolutions for 60 knots forward flight speed. As is evident the rear rotor experiences a significant drop in

the vertical force component due to its interaction with the complex wake flow structures. The asymmetry of the wake flow field also gets reflected on the aerodynamic loads. When the rear rotor is within the wake of the advancing side of the front rotor, significantly higher amplitude oscillations are observed in the vertical force compared to the case when the rear rotor is within the wake of the retreating side of the front rotor.

Using the time histories of the computed forces and moments, average values are calculated using the periodic data obtained after about five revolutions. After having the arithmetical mean of all the forces and moments for both front and rear rotors, the amount of change in the rear rotor with respect to the front rotor is calculated and shown in Figures 5 and 6. The first columns show the results of 60 knots forward flight condition. The results of 80 knots forward flight simulations are presented in the second columns. In each plot, both the effect of the proximity of the rotors and the lateral position of the rear rotor are discussed (case 1 and case 2 simulations which are previously described in Figure 2).

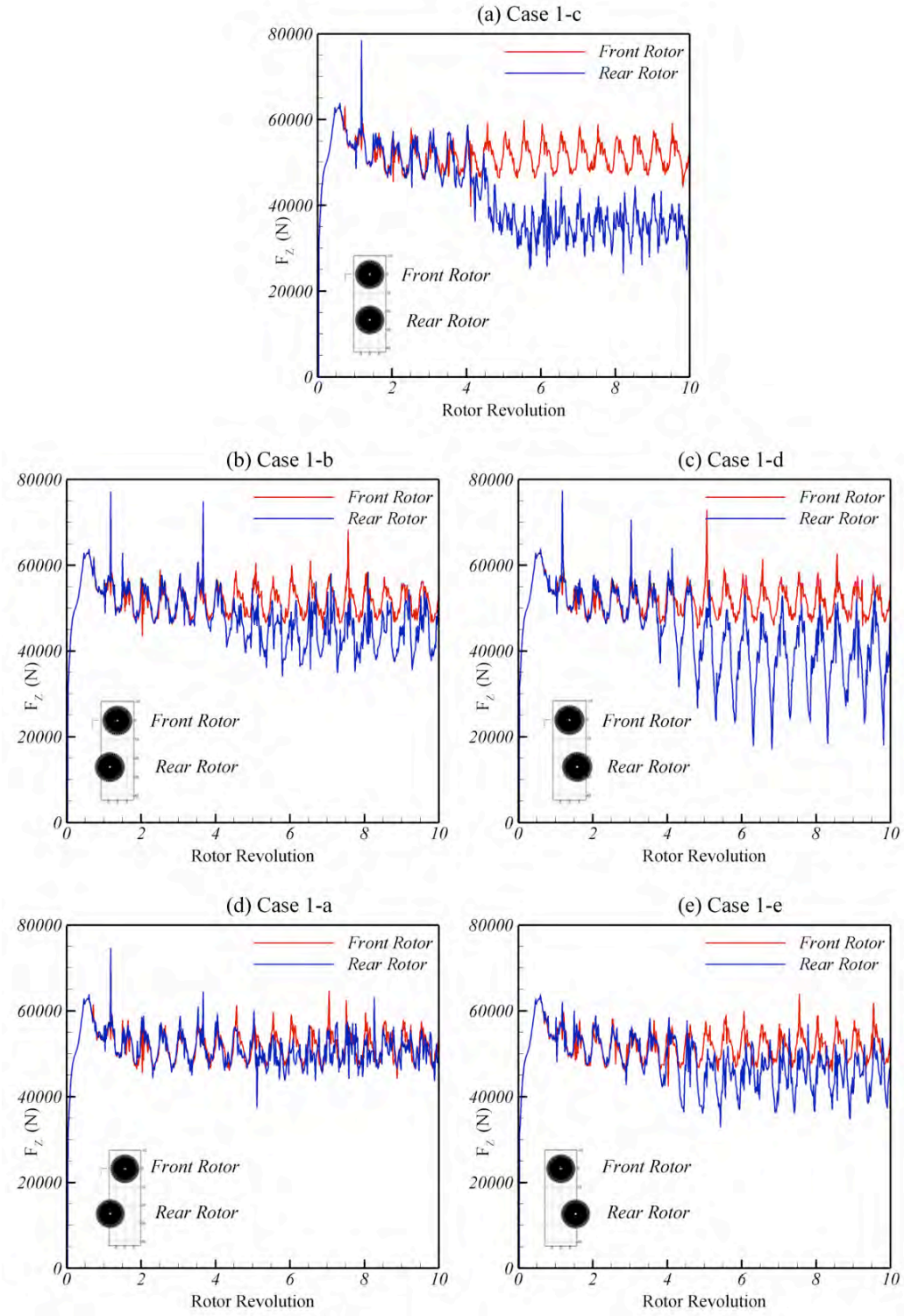

Figure 4. *Vertical force (F_Z) variations for 10 rotor revolutions in 60 knots forward flight when the distance between the hub centers is 24.7 m (a) case 1c (b) case 1b (c) case 1d (d) case 1a (e)case 1e (The cases are described in Figure 1).*

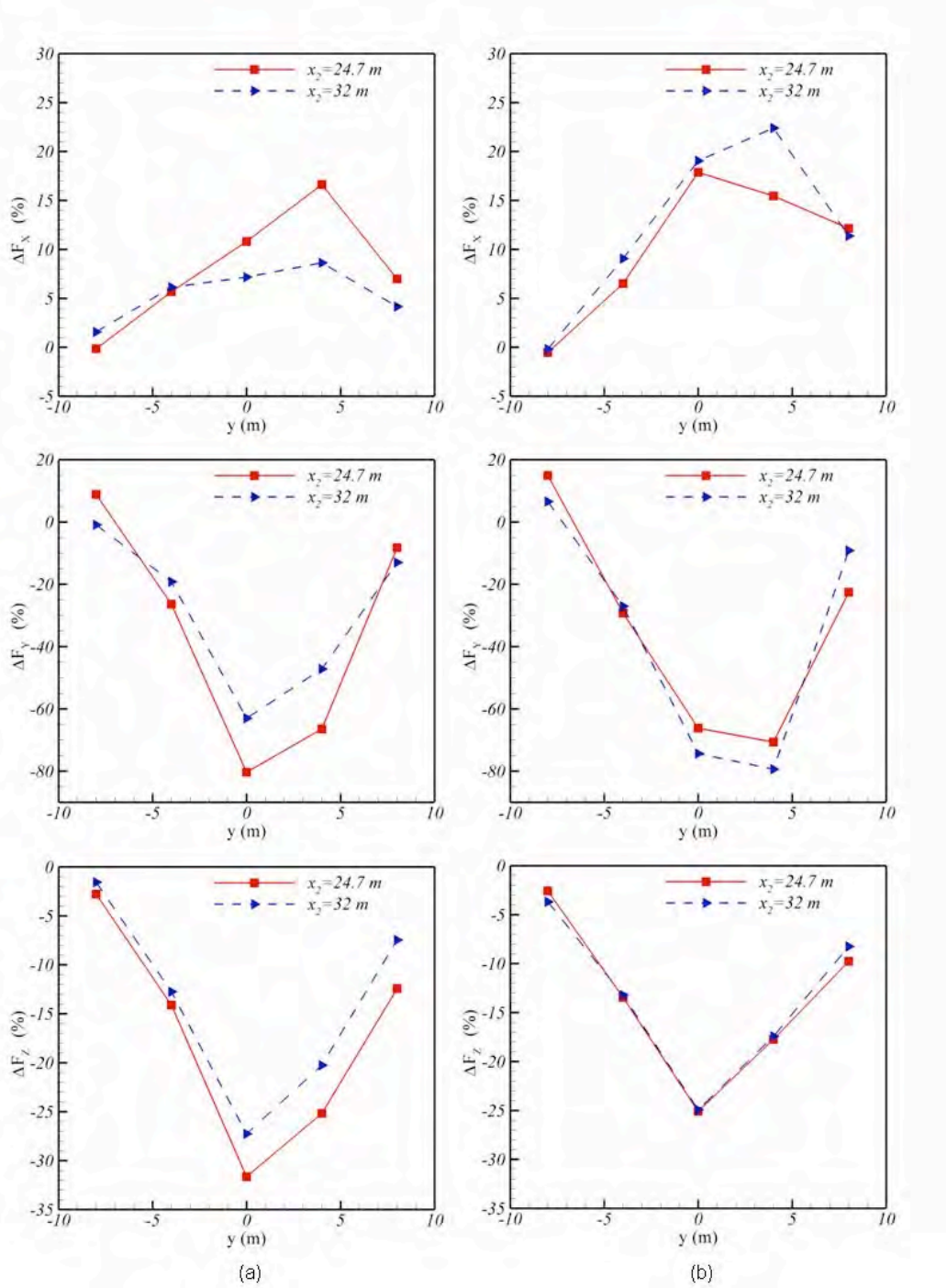

Figure 5. *Percentage change in forces of the rear rotor with respect to the front rotor (a) at 60 knots (b) 80knots*

As can be seen in Figures 5 and 6, case 1 and case 2 simulations produce similar results. The dissimilarities occur due to the intensity of the interactions which differs by the longitudinal distance between the hub centers. As can be seen in Figure 5, F_X of the rear rotor increases with respect to the front rotor. Due to the interactions with the front rotor wake, the velocity field of the rear rotor changes. The rear rotor blades encounter a higher and a complex flow field. The maximum increment in F_X is seen in case 1d. Nearly in all cases F_Y (the side force) of the rear rotor decreases. In 60 knots forward flight the maximum decrease is seen for case 1c simulation. On the other hand, in 80 knots forward flight the maximum decrease is seen for case 1d simulation. The vertical component of the force, F_Z, shows degradation due to the influence of the front rotor wake. For both 60 knots and 80 knots forward flight conditions, maximum decrease occurs in case 1c simulation where the interactions are severe. The decrements are more when the rear rotor is operating at the advancing side rather than the retreating side. Figure 6 shows the amount of changes in moments of the rear rotor. The rolling moment (M_X) decreases in case 1a, 1b and 1c simulations. The amount of decrement is more when the rotors are operating in 80 knots forward flight condition. When the rear rotor operates at the starboard of the front rotor the rolling moments increase. The pitching moment (M_Y) decreases at case 1a, 1b and 1c simulations in 80 knots forward flight. Maximum decrease is seen in case 1a simulation. The rolling moment of the rear rotor increases when operating at the starboard side of the front rotor. Maximum increment is seen in case 1e simulation. On the other hand, at 60 knots forward flight the rolling moment decreases 2% in case 1d and 12% in case 2d. There is an increment in pitching moment in case 1e and

case 2e simulations. The yawing moment of the rear rotor slightly changes in all simulation cases for both 60 knots and 80 knots forward flight as seen in Figure 6.

A frequency analysis of force and moment oscillations is also performed as shown in Figures 7, 8, 9 and 10. The rotational speed of the UH-1H rotor is 324 rpm. Therefore, the rotational and the blade passing frequencies are 5.4 Hz and 10.8 Hz, respectively (UH-1H rotor has two blades). Knowing that the blade advances 6° at each time step during the computations, and therefore, one revolution is completed in 60 time steps (i.e. 60 sample solutions are obtained in one revolution) the sampling rate comes out to be 324 Hz. The frequency axis in these figures extends from zero to half the sampling rate (160 Hz), which was used in performing the Fourier transforms.

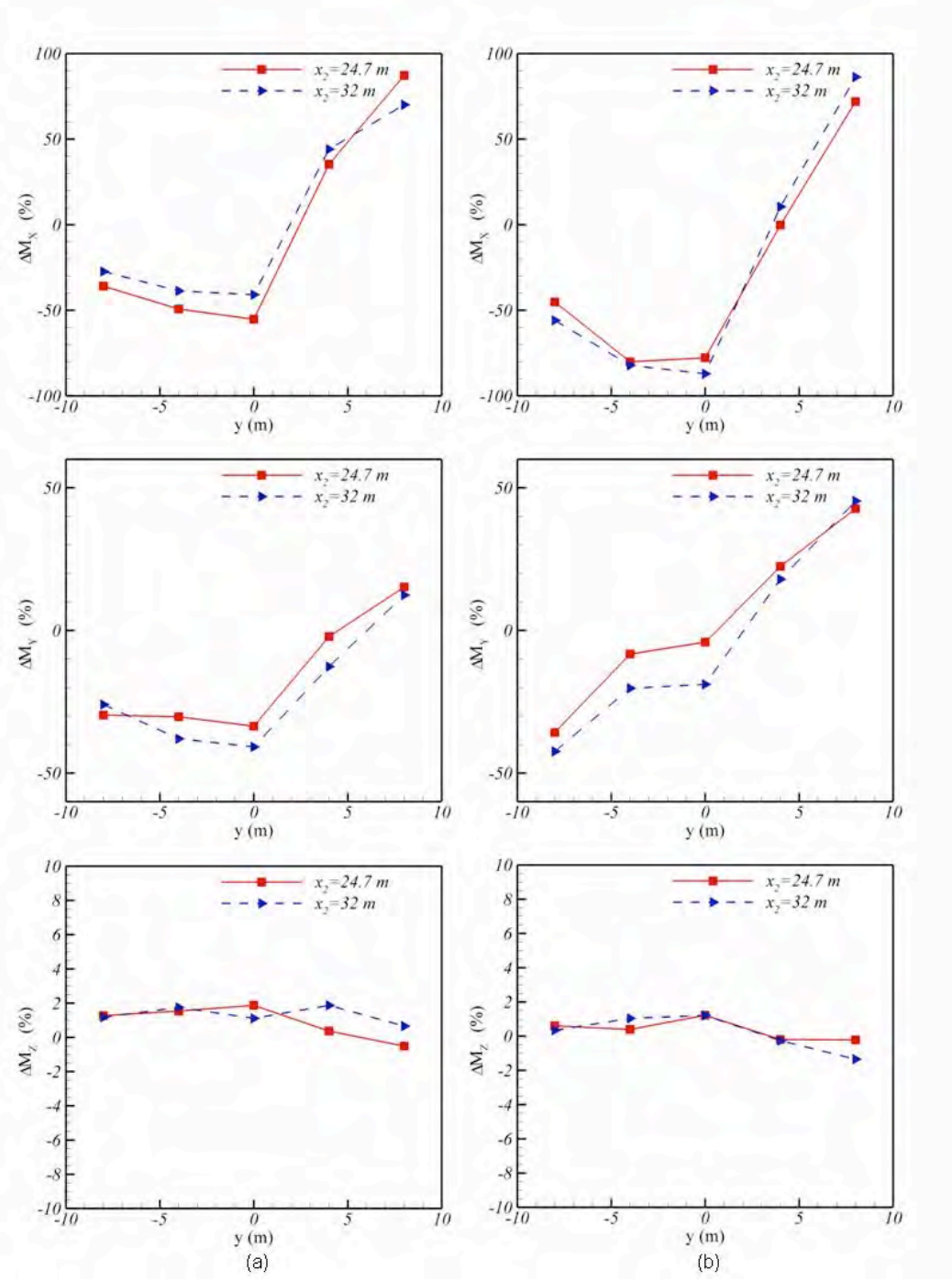

Figure 6. *Percentage change in moments of the rear rotor with respect to the front rotor (a) at 60 knots (b) 80knots*

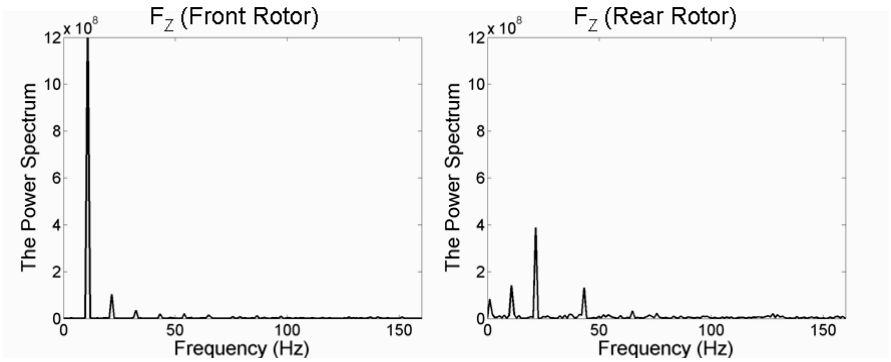

a) Case 1a

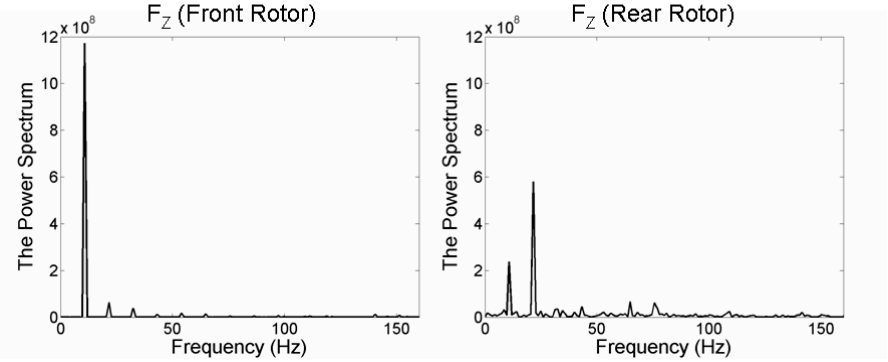

b) Case 1c

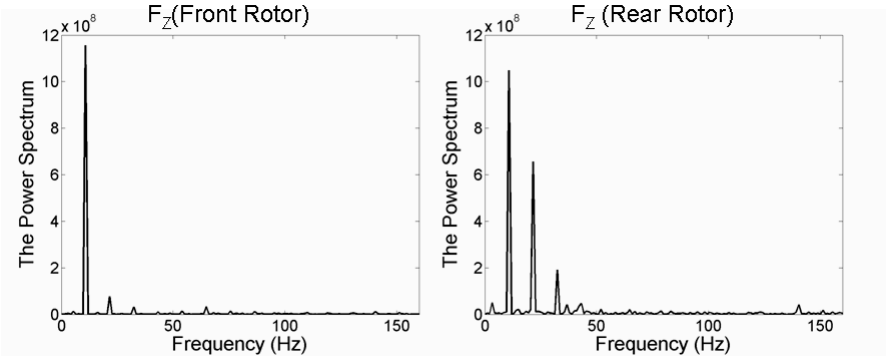

c) Case 1e

Figure 7. *Frequency spectrum of the vertical force (F_Z) for cases 1a, 1c and 1e.*

Figure 7 shows the frequency analysis of the vertical forces (F_Z) for Case 1a, 1c and 1e simulations. Case 1a simulation corresponds to the case when the rear rotor is operating at the retreating side of the front rotor while case 1e simulation corresponds to the case when the rear rotor is operating at the advancing side of the front rotor. The computed performance data showed that in vertical force (F_Z) of the front rotor, the dominant peak occurs at the blade passing frequency which is 10.8 Hz, showing that the interactions have little influence on the performance characteristics of the front rotor. However, due to the effects of interactions, the rear rotor has a dominant peak at the 21.6 Hz, two times the blade passing frequency in case 1a and 1c simulations. It means that the rear rotor is also under the influence of the blade passing frequency of the front rotor. In addition, in Case 1a, a dominant peak is also observed at the fourth harmonic of 43.2 Hz. This harmonic peak is not observed in Cases 1c and 1e. In case 1e simulation, both rotors have a dominant frequency at the blade passing frequency. However, the rear rotor is affected by the interactions, has bigger peaks at the harmonics and unlike Case 1a a peak in the third harmonic is observed instead of the fourth.

Figures 8, 9 and 10 show the frequency spectrum of the rolling (M_X), pitching (M_Y) and yawing (M_Z) moments for both the front and rear rotors. For the rolling moment M_X, both rotors have very similar characteristics, having a dominant peak at the blade passing frequency and less dominant peaks at the harmonics. The pitching moment characteristics on the other hand show significant variations in the sense that the dominant peaks occur at different harmonics and the variations are asymmetric with respect to the centerline. For Cases 1a and 1c the rear rotor dominant peak occurs at two times the blade passing frequency, whereas for Case 1e the dominant peak is at the blade passing frequency. For the yawing moment M_Z the variations are again similar and most of the time the dominant peak only occurs at the blade passing frequency.

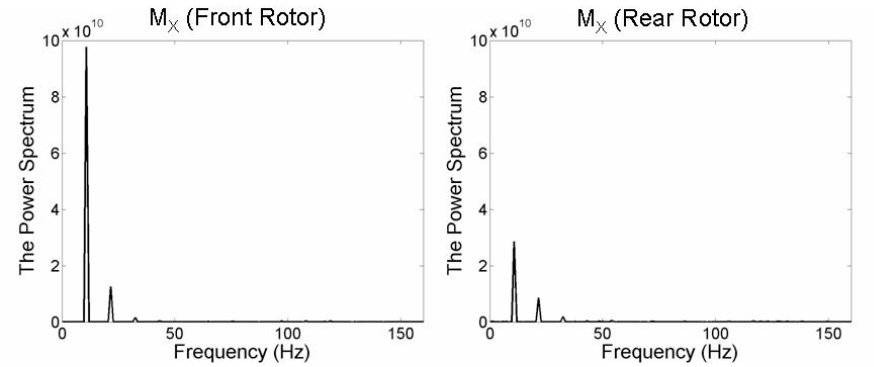

a) Case 1a

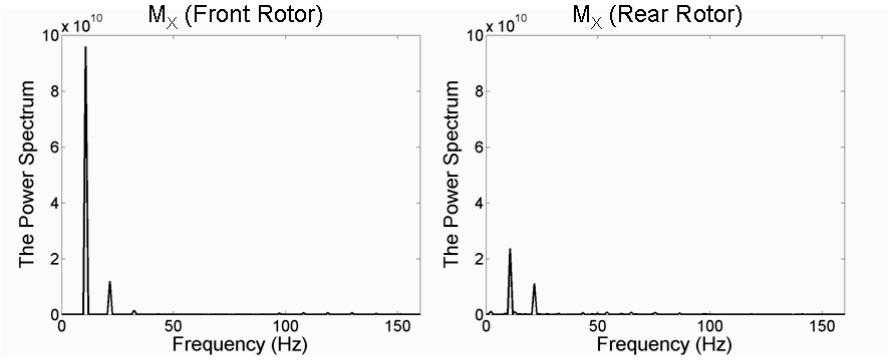

b) Case 1c

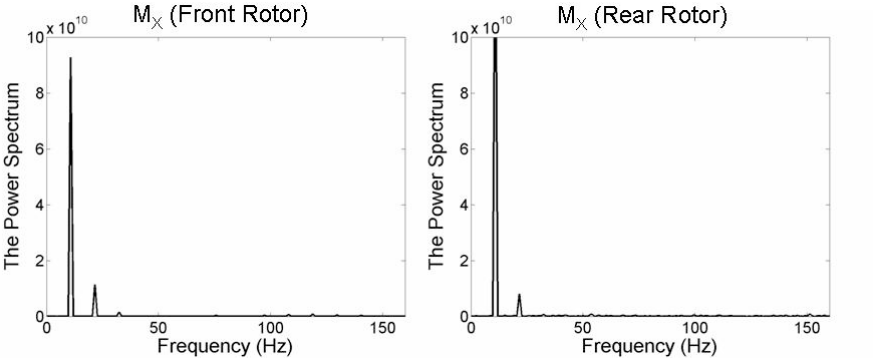

c) Case 1e

Figure 8. *Frequency spectrum of M_X for cases 1a, 1c and 1e.*

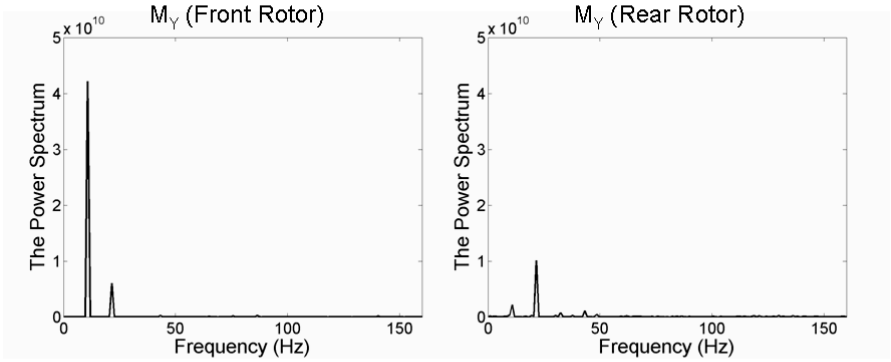

a) Case 1a

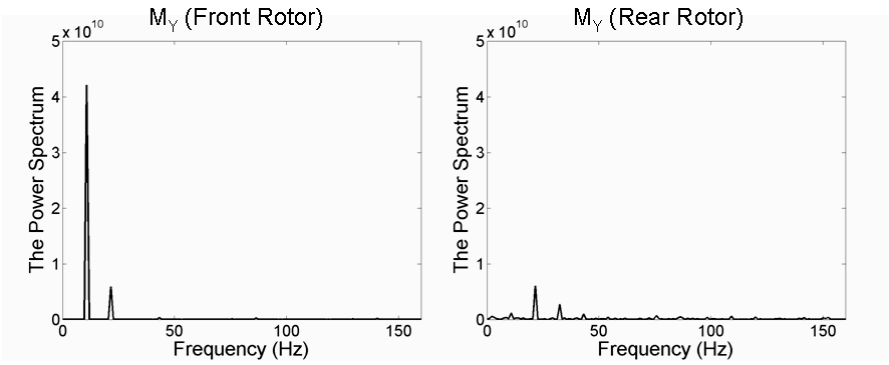

b) Case 1c

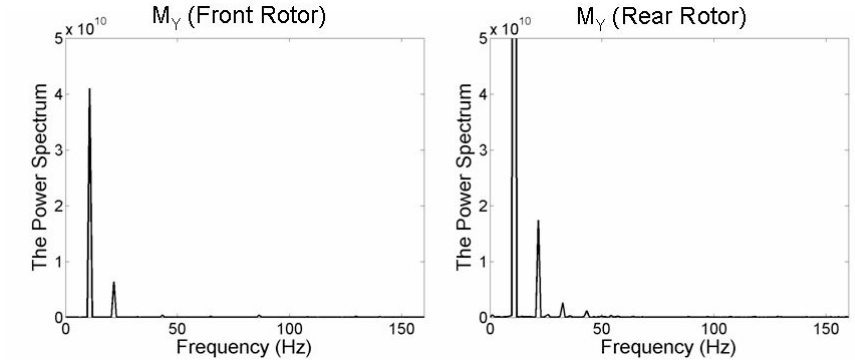

c) Case 1e

Figure 9. *Frequency spectrum of M_Y for cases 1a, 1c and 1e.*

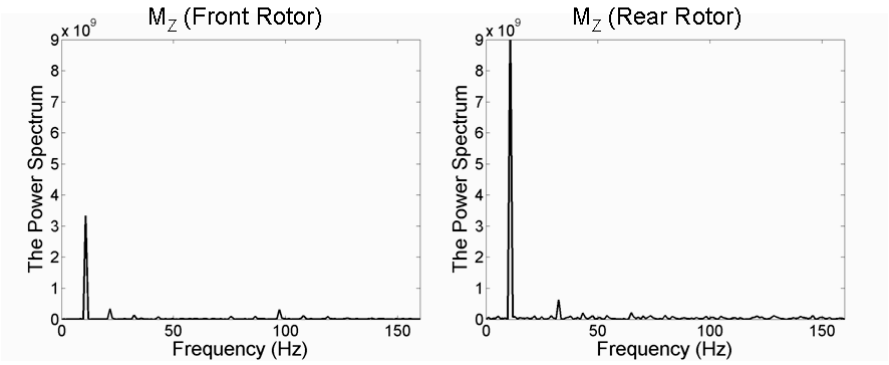

a) Case 1a

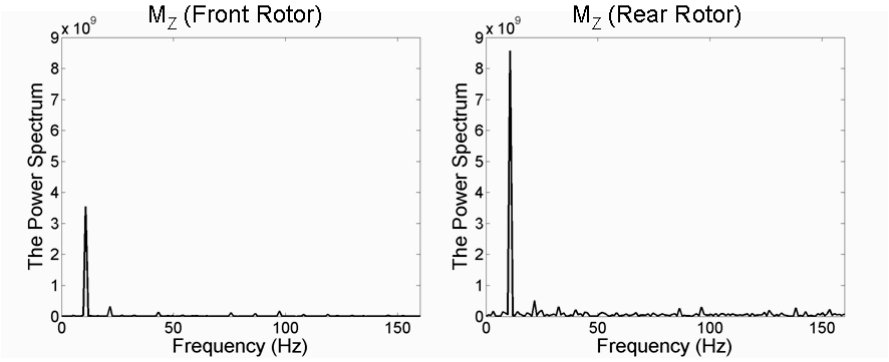

b) Case 1c

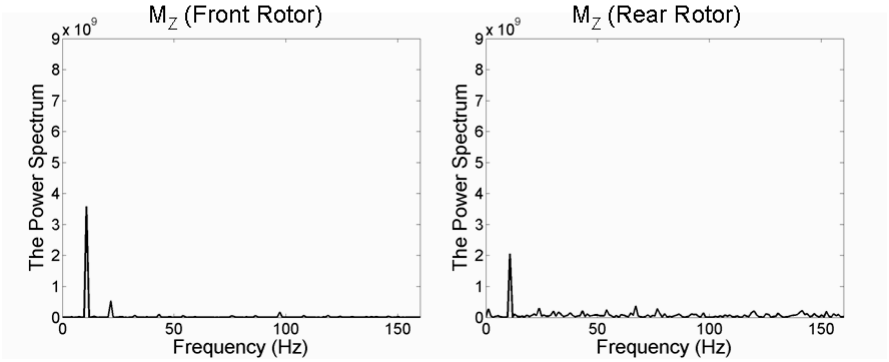

c) Case 1e

Figure 10. *Frequency spectrum of M_Z for cases 1a, 1c and 1e.*

IV. Conclusions

A 3-D unsteady vortex-panel solver based on a free-vortex-wake methodology is used to investigate the rotor-rotor wake interactions of two UH-1H rotors, one operating in the wake flow field of the other, in forward flight. The performance characteristics are analyzed in terms of computed forces and moments on each rotor and their frequency analysis. The rear rotor operates within a complex and vortical free-stream flow due to the interaction of the incoming wake flow. Therefore, wake-rotor interactions cause substantial variations in aerodynamic loads generated by the rear rotor. The asymmetries in the wake geometry in forward flight cause changes in performance characteristics of the rear rotor when it is operating at port and starboard sides of the front rotor. The decrease in vertical lifting is more when the rear rotor is operating within the wake of the advancing side. A frequency spectrum analysis of the force and moment fluctuations of the rear rotor shows that for the vertical force component the rear rotor experiences a dominant peak at two times the blade passing frequency, except when the rear rotor is operating within the wake of the advancing side of the front rotor. Other peaks at different harmonics are also observed and the location of these peaks in the frequency spectrum depends on the lateral position of the rear rotor with respect to the front one. Moment fluctuations generally are similar for the front and rear rotors except for the pitching moment which show fluctuations at two times the blade passing frequency illustrating that the pitching moment gets influenced by the wake interactions more than the other two moment components.

References

1. Leishman, J. G., Bagai, A., "Challenges in Understanding the Vortex Dynamics of Helicopter Rotor Wakes", AIAA Journal, Vol. 36, No. 7, 1998.

2. Bi, N., and Leishman, J. G., “Experimental Study of Rotor/Body Aerodynamic Interactions”, Journal of AAircraft, Vol. 27, No. 9, September 1990.
3. Wilson, J. C., and Mineck, R.E., “Wind –Tunnel Investigation of Helicopter Rotor Wake Effects on Three Helicopter Fuselage Models” NASA TM X-3185,1975
4. Sheridan, P. F., and Smith R. P., “Interactional Aerodynamics- A New Challenge to helicopter Technology”, Journal of American Helicopter Society, Vol. 25, No.1, pp.3-21, January 1980
5. Smith, C. A., and Betzina, M.D., “Aerodynamic Loads Induced by a Rotor on a Body of Revolution” Journal of American Helicopter Society, Vol. 31, No.1, 1986, pp. 29-36
6. McMahon, H. M., Komerath, N. M., and Hubbard, J. E., “ Studies of Rotor-Airframe Interactions in Forward Flight” AIAA Paper 85-5015, October 1985
7. Wilby, P. G., Young, C., and Grant, J. “ An Investigation of the Influence of Fuselage flow Field on rotor Loads and the Effects of Vehicle Configuration” Vertica, Vol. 3, 1979, Pergamon Press Ltd., UK
8. Betzina, M. D., Smith, C. A., and Shinoda, P., “Rotor/Body Aerodynamic Interactions”
9. Fletcher, T. M., Brown, R. E., “Main rotor – Tail Rotor Wake Interaction and its Implications for Helicopter Directional Control”, Proceedings of the 32nd European Rotorcraft forum, Maastricht, Netherlands, 2006.
10. Meakin, RL., “Moving Body Overset Grid Methods for complete tilt-rotor simulations”, AIAA Paper 93-3350-CP, Presented at the 11th AIAA Computational Fluid Dynamics Conference, Orlando, FL, July 1993.
11. Akimov, A. I., Butov, V. P., Bourtsev, B. N., and Selemenev, S. V., “Flight Investigation of Coaxial rotor Tip Vortex Structure”, Proceedings of the American Helicopter Society, Alexandria, VA, 1994, pp. 1431-1449.
12. Bagai, A., and Leishman, J. G., “Free-Wake Analysis of Tandem, Tilt-Rotor and Coaxial Rotor Configurations,” Journal of the American Helicopter Society, Vol.41, No. 3, July 1996, pp.196-207.
13. Brown, R. E. “Rotor Wake Modeling for Flight Dynamic Simulation of Helicopters” AIAA Journal, Vol. 38, No. 1, January 2000.
14. Katz, J. and Plotkin, A., Low-Speed Aerodynamics: From Wing Theory to Panel Methods, McGraw-Hill, Inc., 1991.
15. Vatistas, G.H., Kozel, V., and Mih, W.C., 1991, “A Simpler Model for Concentrated Vortices,” Experiments in Fluids, Vol. 11.
16. Scully, M.P., 1975, “Computation of Helicopter Rotor Wake Geometry and Its Influence on Rotor Harmonic Airloads,” ASRL TR 178-1.
17. Lamb, Sir Horace, Hydrodynamics, 6th Edition, pp. 592-593, 668-669, Cambridge University Press, 1932.
18. Yemenici, O., 2009, “Investigation of Rotor Wake Interactions in Helicopters Using 3D Unsteady Free Vortex Wake Methodology,” MS Thesis, Middle East Technical University.
19. Yemenici, O., Sezer-Uzol, N., Uzol, O., 2010, “Investigation of Rotor-Rotor Interactions for Two Helicopters in Forward Flight using Free-Vortex Wake Methodology,” 28th AIAA Applied Aerodynamics Conference, 28 June – 1 July 2010, Chicago, Illinois.
20. Sezer-Uzol, N., Uzol, O., “Effect of Steady and Transient Wind Shear on the Wake Structure and Performance of a Horizontal Axis Wind Turbine Rotor,” Proceedings of 47th AIAA Aerospace Sciences Meeting, 5 - 8 Jan 2009, Orlando World Center Marriott, Orlando, Florida.
21. Tarimci, O., Yilmaz, D., and Yavrucuk I., “On the Level of Center of Gravity Modeling Error in Neural Network Based Adaptive Controller Design”, 2008.
22. Caradonna, F. X. and Tung, C., Experimental and Analytical Studies of a Model Helicopter Rotor in Hover, NASA TM-81232, 1981